



THE UNIVERSITY *of* EDINBURGH

Edinburgh Research Explorer

## IFITM proteins inhibit HIV-1 protein synthesis

**Citation for published version:**

Lee, W-YJ, Fu, RM, Chen, L & Sloan, RD 2018, 'IFITM proteins inhibit HIV-1 protein synthesis', *Scientific Reports*, vol. 8, 14551. <https://doi.org/10.1038/s41598-018-32785-5>

**Digital Object Identifier (DOI):**

[10.1038/s41598-018-32785-5](https://doi.org/10.1038/s41598-018-32785-5)

**Link:**

[Link to publication record in Edinburgh Research Explorer](#)

**Document Version:**

Publisher's PDF, also known as Version of record

**Published In:**

Scientific Reports

**General rights**

Copyright for the publications made accessible via the Edinburgh Research Explorer is retained by the author(s) and / or other copyright owners and it is a condition of accessing these publications that users recognise and abide by the legal requirements associated with these rights.

**Take down policy**

The University of Edinburgh has made every reasonable effort to ensure that Edinburgh Research Explorer content complies with UK legislation. If you believe that the public display of this file breaches copyright please contact [openaccess@ed.ac.uk](mailto:openaccess@ed.ac.uk) providing details, and we will remove access to the work immediately and investigate your claim.



# SCIENTIFIC REPORTS

OPEN

## IFITM proteins inhibit HIV-1 protein synthesis

Wing-Yiu Jason Lee<sup>1</sup>, Rebecca Menhua Fu<sup>2</sup>, Chen Liang<sup>3</sup> & Richard D. Sloan<sup>1,2,4</sup>

**Interferon induced transmembrane proteins (IFITMs) inhibit the cellular entry of a broad range of viruses, but it has been suspected that for HIV-1 IFITMs may also inhibit a post-integration replicative step. We show that IFITM expression reduces HIV-1 viral protein synthesis by preferentially excluding viral mRNA transcripts from translation and thereby restricts viral production. Codon-optimization of proviral DNA rescues viral translation, implying that IFITM-mediated restriction requires recognition of viral RNA elements. In addition, we find that expression of the viral accessory protein Nef can help overcome the IFITM-mediated inhibition of virus production. Our studies identify a novel role for IFITMs in inhibiting HIV replication at the level of translation, but show that the effects can be overcome by the lentiviral protein Nef.**

As viruses depend on cells to complete their replication cycles, this has driven the evolution of a series of antiviral factors that directly subvert viral replication within cells. Recent work has revealed the striking scale of antiviral mechanisms employed by cells - almost every step of viral replication is apparently targeted by host encoded antiviral factors. For HIV the best defined examples are APOBEC3G/3F and SAMHD1 that inhibit viral reverse transcription, TRIM5 $\alpha$  that targets viral capsid uncoating, and tetherin that prevents viral egress (reviewed in<sup>1,2</sup>). However, genomic and proteomic screens can aid identification of further antiviral factors, and so there is an expanding list being described<sup>3,4</sup>. Such studies identified the MxB/Mx2 protein that targets HIV-1 replication around nuclear entry<sup>5,6</sup>, and the SERINC3 and SERINC5 proteins that target HIV-1 entry<sup>7,8</sup>.

The interferon induced transmembrane proteins (IFITMs) have been similarly identified in multiple independent screens as antiviral factors<sup>9–12</sup>. Humans have three antiviral IFITMs - IFITM1, IFITM2 and IFITM3 (reviewed in<sup>13</sup>). IFITM expression inhibits viral entry into cells<sup>9,10</sup>, a phenotype that is enhanced by incorporation of IFITM proteins into viral particles<sup>14–16</sup>. Inhibition of viral entry is thought to occur via IFITM-mediated changes in the physical characteristics of the host cell membrane thereby inhibiting virus-cell membrane fusion<sup>17</sup>, though other inhibitory mechanisms affecting entry have been proposed<sup>18</sup>. By employing this generic inhibitory mechanism, IFITMs can then inhibit the entry of a broad range of viruses including influenza A virus, hepatitis C virus, Ebola virus, SARS coronavirus, Dengue virus, Zika virus, and HIV-1<sup>9,10,19–21</sup>. Of note, the block to HIV-1 entry by IFITM proteins seems to depend on virus co-receptor use, with CCR5-tropic strains typically more sensitive to IFITM1 while CXCR4-tropic strains are typically more sensitive to IFITM2 and IFITM3<sup>16,22,23</sup>.

Yet since the discovery of their antiviral effect upon HIV-1, it was immediately apparent that a viral replication step downstream of host genome integration might also be inhibited by IFITM proteins, as IFITM1 knockdown increased HIV-1 titres from infected CD4<sup>+</sup> T-cells with a CXCR4-tropic virus that would be resistant to entry inhibition<sup>10</sup>. In the same study, IFITM1 inhibited the replication of HIV-1 in T-cell culture despite the evidence that IFITM1 had no effect on viral replication steps from cell entry to host genome integration for the CXCR4-tropic viral strain used. Other studies have also noted IFITM1–3 expression consistently reduces viral particle production from cells<sup>12,14–16,23–27</sup>. When this occurs, IFITM expression is typically associated with reductions in HIV-1 Gag levels, implying a block in viral protein synthesis that is independent from inhibition of virus entry.

Despite the frequency of these observations, there has been little or no attempt to explain them. Why viral production should be affected by IFITM expression is unclear. We therefore sought to investigate the potential block in protein synthesis induced by IFITMs and now show that IFITM expression leads to an inhibition of lentiviral production, which for HIV-1 occurs due to specific exclusion of viral mRNA from polysomes. Yet we also find that expression of the lentiviral accessory protein Nef can help relieve the inhibition in virus production,

<sup>1</sup>Blizard Institute, Barts and The London School of Medicine and Dentistry, Queen Mary University of London, London, E1 2AT, United Kingdom. <sup>2</sup>Division of Infection and Pathway Medicine, School of Biomedical Sciences, University of Edinburgh, Edinburgh, EH16 4SB, United Kingdom. <sup>3</sup>McGill University AIDS Centre, Lady Davis Institute, Montreal, Quebec, H3T 1E2, Canada. <sup>4</sup>ZJU-UoE Institute, Zhejiang University, Haining, Zhejiang, 314400, P.R. China. Correspondence and requests for materials should be addressed to R.D.S. (email: [richard.sloan@ed.ac.uk](mailto:richard.sloan@ed.ac.uk))

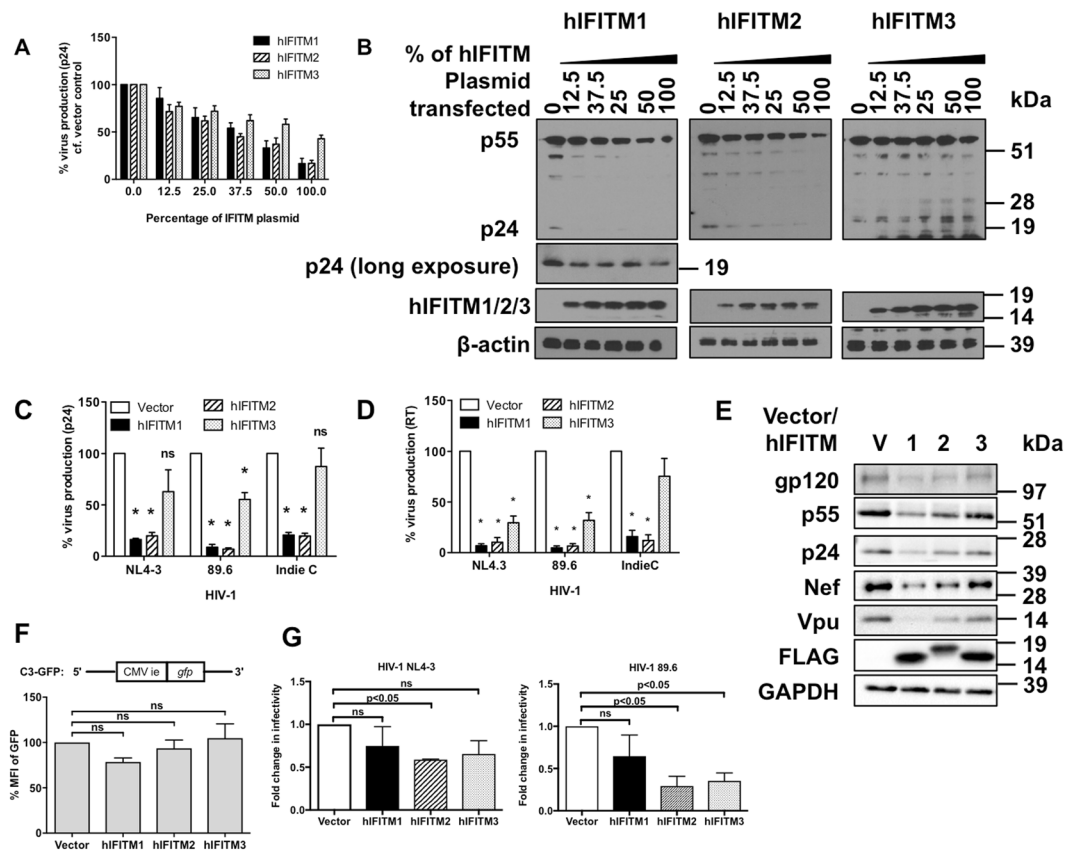


**Figure 1.** IFITMs inhibit HIV viral output and viral protein production in transfected cells. HEK293T cells were transfected with a titration of expression vectors for FLAG tagged IFITMs, with the total quantity of 0.5  $\mu$ g, plus 0.5  $\mu$ g of HIV-1 NL4-3 proviral DNA. (A) Levels of virus production were measured by p24 ELISA 48 h post-transfection, and (B) intracellular viral proteins and IFITMs were analyzed by immunoblotting. HEK293T cells were transfected with 0.5  $\mu$ g of FLAG-tagged IFITM expression vectors and 0.5  $\mu$ g of HIV-1 NL4-3 proviral DNA. Levels of virus production from indicated HIV-1 proviral DNAs were measured by (C) p24 ELISA and (D) reverse transcriptase (RT) activity assay and (E) immunoblotting of intracellular proteins 48 h post-transfection. (F) Mean fluorescence intensity (MFI) of GFP expression in HEK293T cells co-transfected with 0.5  $\mu$ g CMV-driven GFP vector and 0.5  $\mu$ g IFITM-expression vectors or empty vectors measured by flow cytometry 48 hours post-transfection. (G) HIV-1 NL4-3 and 89.6 viruses were produced from HEK293T cells transfected with vector or the indicated IFITMs in TZM-bl cells for 48 hours. Infectivity in TZM-bl cells was measured by luciferase activity assay 48 hours after infection with virus stock with equivalent p24 concentration. Data show mean  $\pm$  S.E.M. of more than 3 independent experiments. All differences were assessed with Student's t-test and \*indicates  $p < 0.05$ .

allowing HIV-1 to better replicate in the presence of IFITM proteins. Thus IFITM proteins are able to inhibit HIV-1 replication through three distinct processes - inhibition of viral entry, reduction of viral particle infectivity, and inhibition of viral protein synthesis.

## Results

**IFITMs inhibit HIV-1 production.** We first wanted to confirm if IFITMs affect the production of HIV from virus producing cells as noted in previous reports<sup>10,12,14–16,23–27</sup>. We used a co-transfection scheme in which we co-transfected HEK293T cells with plasmids containing HIV-1 proviral DNAs together with expression vectors encoding human IFITM1–3, allowing the effects on virus production to be studied independently of effects of IFITM proteins on viral entry. The quantity of virus produced was then analyzed by supernatant p24 ELISA and reverse transcriptase activity assays. Increasing levels of IFITM expression decreased HIV-1 NL4-3 output in a concentration-dependent manner consistent with loss of intracellular p55 and p24 levels (Fig. 1A,B), with a similar decrease seen in supernatant when both p24 concentration (Fig. 1C) and reverse transcriptase activity (Fig. 1D) were measured. Notably, the expression of IFITM1 and IFITM2 reduced the HIV-1 output while the effect was weaker for IFITM3. We then studied the effect of IFITMs on other viral proteins, and found IFITM1 and IFITM2 expression led to a reduction in the levels of all HIV-1 NL4-3 proteins assayed in transfected cells (Fig. 1E). Similar to HIV-1 NL4-3, viral production from the HIV-1 plasmid proviral DNAs 89.6 and Indie-C1 was also reduced by IFITM expression (Fig. 1C,D).

In addition to HIV-1, the expression of IFITMs also reduced the quantity of virus produced from cells transfected with plasmid proviral DNAs for HIV-2 and SIVs (Fig. S1A and S1B). Of note, HIV-2<sub>ROD</sub> and SIV<sub>AGM</sub> appeared to be less susceptible to this IFITM-mediated effect compared to the HIV-1 viruses studied. We also found similar inhibitory effects upon HIV-1 with transfected African Green Monkey IFITM1 (Fig. S1C).

We were concerned however that the loss of viral production we saw might be due to generic inhibition of protein production during IFITM expression, but detection of GFP from a transfected reporter plasmid as measured by flow cytometry was not significantly affected by IFITM expression (Fig. 1F). While similar experiments using a plate reader showed even highly overexpressed IFITMs minimally affected GFP levels (Figure S2A), suggesting the strong inhibition in virus production we observed (Fig. 1A–E) might be specific. Further, expression of GFP or control vector did not influence virus production (Figure S2B–C) or IFITM activity (Figure S2D–E) suggesting the block to virus production is not due to generic overexpression artefact. We also measured the infectivity of the virus produced from IFITM-expressing cells, in TZM-bl cells and showed that virus produced have lower infectivity (Fig. 1G), in agreement with previous results<sup>14–16</sup>.

We noted that levels of IFITM proteins in transfected HEK293T cells were often higher than those seen in type-I interferon treated CD4<sup>+</sup> T-cells and monocyte derived macrophages (MDMs) (Figure S3) and so we next investigated the influence of IFITM proteins in cells in which levels of expression could be inducibly expressed. We also wanted to test if IFITMs inhibit viral production in infected cells rather than provirus transfected cells. As such we infected SupT1 cells expressing doxycycline inducible IFITM1–3 with wild type NL4-3 virus<sup>10</sup>. To avoid the well documented inhibition of virus entry by IFITMs playing a role in our experiments, after spinoculation, unbound virus was washed off and cells were resuspended in new medium containing doxycycline and the CXCR4 antagonist AMD3100 to induce IFITM expression only after virus entry and to limit viral replication to a single round respectively. Complete entry blockade by AMD3100 was confirmed with pre-treatment of cells (Figure S3A). The quantity of wild type HIV-1 produced by IFITM-expressing T-cells was inhibited across a range of viral inputs (Fig. 2A) and was paired with losses in all viral protein levels (Fig. 2B,C). Though collectively this indicates that IFITMs inhibit viral production independent of their effects on viral entry. Notably, the levels of doxycycline induced IFITM were similar to those found in type I interferon treated CD4<sup>+</sup> T-cells and monocyte derived macrophages (Figure S3B, C,E).

We next wished to investigate this effect using knockdown of endogenous IFITM levels to avoid overexpression artefact, and to assess the relative contribution of IFITMs towards inhibition of viral production that is observed with type I interferon (IFN) treatment. We therefore analyzed viral output from HIV-1 NL4-3 plasmid proviral DNA transfected and IFN- $\beta$  treated TZM-bl cells that had been transduced with shRNAs targeting different IFITMs<sup>28</sup>. Infection of cells with virus produced during transfection was inhibited through the use of the CXCR4 antagonist AMD3100, and thus the level of viral output in our analysis cannot be confounded by entry inhibition due to IFITM expression. The efficiency of knockdown in IFITM expression was confirmed by immunoblotting using monoclonal antibodies specific for individual IFITMs (Fig. 3A). As anticipated, IFN- $\beta$  treatment reduced viral production in HIV-1 transfected TZM-bl cells (Fig. 3B). Despite some weak knockdown cross-reactivity, such that shRNA targeting IFITM1 caused weak knockdown of IFITM2 (Fig. 3A), and that it was not possible to knockdown IFITM3 in isolation, knockdown of both IFITM1 and IFITM2 clearly rescued the level of virus produced in IFN- $\beta$  treated cells (Fig. 3C). Further, knockdown of all three IFITMs gave a higher rescue, indicating that the inhibitory effects of IFITM1 and IFITM2 on viral production are perhaps non-redundant in the context of HIV-1 replication. These effects were paired with rescue of all viral protein levels during IFITM knockdown (Fig. 3D,E). Knockdown of IFITMs rescued viral protein production by around 1.5 to 3.5 fold, and so is concordant with viral production rescue of 2.0 to 2.5-fold. These data then show that endogenous levels of IFITMs can inhibit viral particle output and that our prior results in HEK293T transfections and SupT1 infections are not an overexpression artefact. They also suggest that IFITMs are a significant component of the antiviral response induced by type I interferon, as the 7-fold restriction of virus production seen on IFN- $\beta$  (Fig. 3B) can be reduced to 3.5-fold upon IFITM1–3 knockdown (Fig. 3E).

We next sought to confirm if the knockdown of physiologically relevant levels of IFITMs in HIV-1 infected primary cells could rescue viral protein production. Primary human CD4<sup>+</sup> T cells were infected with HIV-1 following transduction with lentiviral particles for the expression of shRNAs targeting different IFITMs. Transduction with one shRNAs resulted in a specific ~90% downregulation of IFITM2 (though combined with IFITM1 and IFITM3 upregulation), while another shRNA led to a ~50% downregulation of all three IFITMs (Fig. 4A–C). We were unable to specifically knockdown IFITM1 with reasonable efficiency. To mitigate the effects of IFITMs inhibiting viral entry on our studies of inhibited viral production, we took advantage of recent observations showing that different IFITM proteins vary in their inhibition of viral entry depending on HIV-1 co-receptor usage<sup>16,22,23</sup>. IFITM1 inhibits entry of CCR5-tropic viruses and IFITM2/3 predominantly inhibits CXCR4-tropic viruses. We therefore studied viral production effects driven by IFITM2 and IFITM3 with dual-tropic HIV-1 89.6, wherein cells were treated with the CXCR4 antagonist AMD3100 prior to and during infection. AMD3100 treatment would direct viral entry via CCR5 due to CXCR4 blockade and thus mitigate entry inhibition by either IFITM2 or IFITM3. We used intracellular p24 staining of infected cells in single cycle infections to measure uptake of virus after infection with trypsin treatment to remove cell surface bound virus (Figure S4)<sup>29–31</sup>. Although cellular uptake of viral p24 is not an exact measure of virus entry due to the uptake of virus into potentially non-productive endocytic pathways, p24 uptake is commonly found to be inhibited by IFITM expression<sup>14,15,25,26</sup>, while endocytic uptake of virus occurs at a lower rate in primary CD4<sup>+</sup> T-cells<sup>32</sup>. We confirmed that viral uptake was minimally impeded with these during IFITM knockdown (Fig. 4D,E), consistent with prior observations<sup>22</sup>. Therefore reductions in virus production were considered to arise predominantly from IFITM-driven effects other than inhibition of viral entry. As such knockdown of IFITM2 led to a clear rescue of viral particle output (7-fold, Fig. 4F) that was coupled with rescue in viral protein expression (Fig. 4G,H), though this was in the context of somewhat elevated IFITM1 and IFITM3 levels (Fig. 4A). Similarly, knockdown

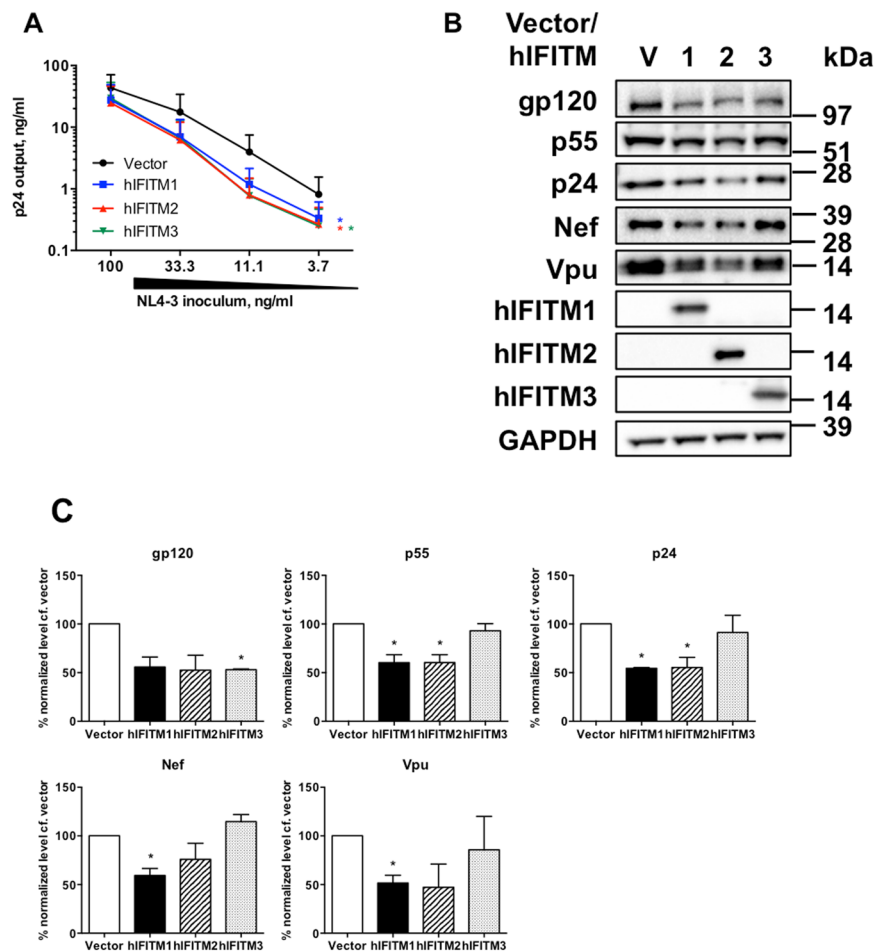


**Figure 2.** Inducible expression of IFITMs after viral entry inhibits HIV viral output and viral protein production in infected SupT1 cells. (A) SupT1 cells were infected with the indicated dilutions of wild type HIV-1 NL4-3 inoculum and then treated with 1  $\mu$ g/ml doxycycline to induce IFITMs post-entry and 5  $\mu$ M AMD3100 to limit infection to a single cycle. At 72 h post-infection levels of virus production were measured by p24 ELISA and differences assessed by Two-way ANOVA with Bonferroni's multiple comparison test. (B) Cellular viral proteins and IFITMs were analyzed by immunoblotting and (C) densitometry. Data show mean  $\pm$  S.E.M. of 3 independent experiments. Differences were assessed with Student's t-test and \*indicates  $p < 0.05$ .

of IFITM1–3 led to rescue of viral protein production and viral particle output ( $>10$ -fold) (Fig. 4F). Though IFITM1 which was depleted in this experiment can inhibit R5-tropic virus entry, thus a proportion of this latter result for IFITM1–3 may be attributable to weak IFITM1 driven entry inhibition, which was not the case for our data surrounding IFITM2-driven block to virus production. That inhibition of virus uptake was measurably weak (Fig. 4D,E) suggests that viral production inhibition may be the dominant form of IFITM driven inhibition in this experiment. Overall, this confirms that physiologically relevant levels of IFITM proteins can clearly inhibit HIV-1 production in primary cells independent of their effects upon entry and infectivity, that this is not an overexpression artefact, and occurs in a manner that is consistent with our observations in cell lines.

**IFITMs restrict HIV-1 protein synthesis.** As we found that IFITM expression was associated with losses in viral protein production and viral output, we next asked if IFITMs play a role in inhibiting the transcription or stability of viral mRNA by analyzing the level of unspliced, singly-spliced, and multiply-spliced transcripts detected by RT-qPCR from total RNA of whole cell lysates. IFITM1 and IFITM2 weakly reduced the levels of singly-spliced and multiply-spliced transcripts, while IFITM3 had no measureable effect (Fig. 5A). The total level of unspliced transcripts remained unaffected in the presence of IFITM proteins (Fig. 5A) but nonetheless there were reductions of intracellular level of Gag (a product of unspliced transcripts) in our prior analyses (Figs 1–4). This prompted us to investigate if IFITM proteins affect translation of viral transcripts.

To achieve this we performed a polysome analysis for HIV-1 transcripts during IFITM expression. We first analyzed the RNA content in cell lysates fractionated on a sucrose gradient by ultracentrifugation. The total RNA profiles (Fig. 5B) recovered from selected fractions of virus producing cells expressing IFITMs are comparable to vector-transfected control, suggesting that IFITM expression did not alter global translation in the cell.



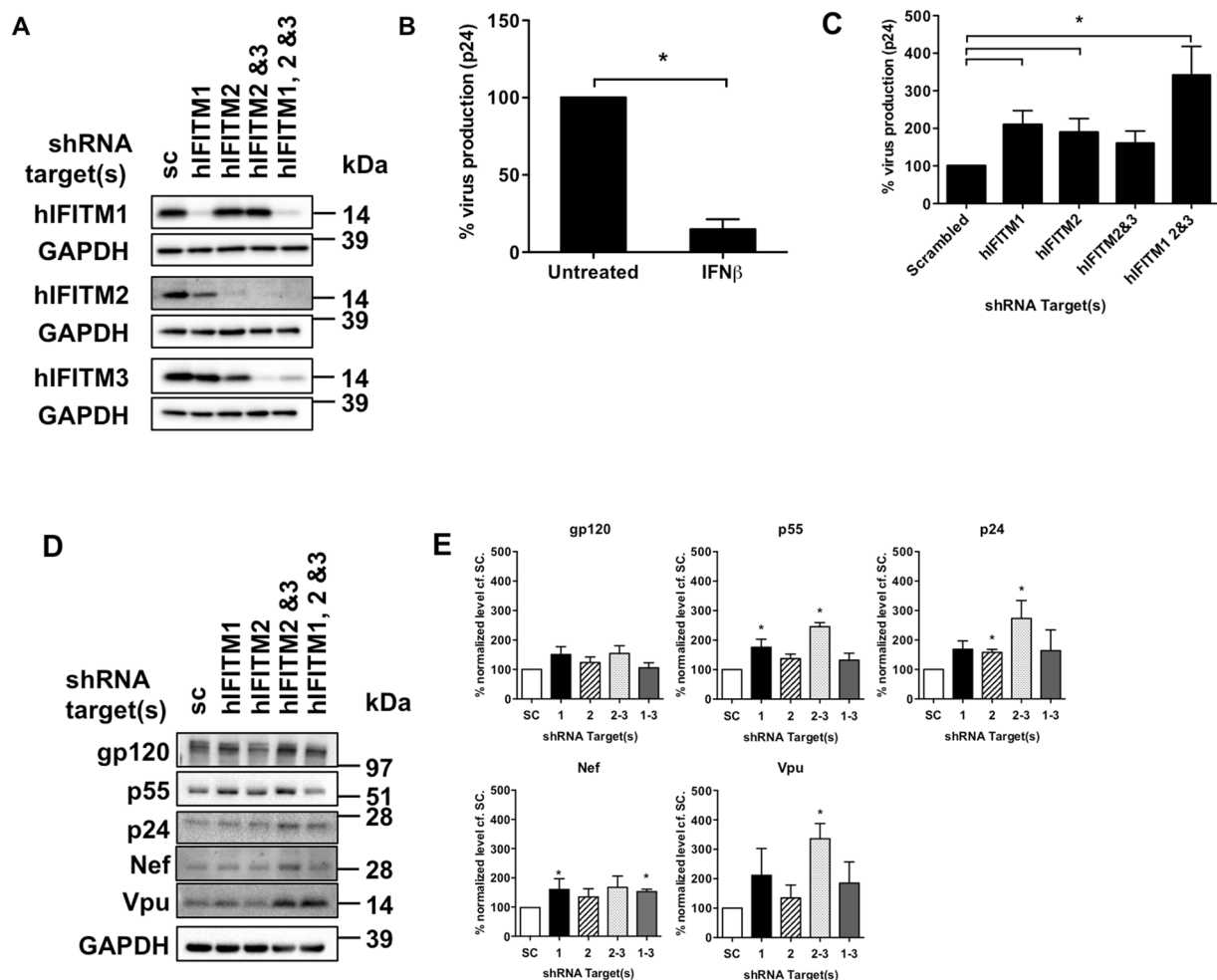


**Figure 3.** Knockdown of IFITMs rescues HIV-1 output and viral protein production in TZM-bl cells. TZM-bl cells transduced with shRNAs against the indicated IFITMs or scrambled control (sc) were treated with 100IU/ml IFN $\beta$  for 72 hours. **(A)** Levels of IFITM expression were analyzed by immunoblotting. **(B)** Scrambled control TZM-bl cells were transfected with HIV-1 NL4-3 proviral DNA and treated with AMD3100 and 100IU/ml IFN $\beta$  for 4h post-transfection. Level of virus production was measured by p24 ELISA 72 h post-transfection. TZM-bl cells transduced with shRNAs against the indicated IFITMs or scrambled control were transfected with HIV-1 NL4-3 proviral DNA and then treated with AMD3100 and IFN $\beta$  4h post-transfection. Level of virus output and viral proteins was measured by **(C)** p24 ELISA and **(D)** immunoblotting, respectively, at 72 hours post-transfection. **(E)** Immunoblotting was further analyzed by densitometry. Data show mean  $\pm$  S.E.M. of 3 independent experiments. Differences were assessed with Student's t-test and \*indicates  $p < 0.05$ .

We used the level of ribosomal protein L7 as a guide for selection of fractions in our analysis (Fig. 5C) as it is a component of 60S ribosomes, which are enriched in 80S monosomes (such as fraction 10 Fig. 5C) as well as polysomes (such as fractions 14–18). The levels of GAPDH mRNA were not reduced in polysome fractions (Fig. 5D). Reductions in the levels of viral transcripts in polysome fractions (in contrast to whole cell lysates – Fig. 5A) would indicate specific translational inhibition. As such, we analyzed the level of viral transcripts in selected fractions covering the whole RNA profile with RT-qPCR. IFITM1 and IFITM2 significantly reduced the level of unspliced and singly-spliced viral transcripts in polysomes (Fig. 5E,F) and increased the level of these transcripts in the ribosome-free fraction (fraction 6), suggesting that expression of IFITM1 and IFITM2 inhibited translation of these viral transcripts. IFITM1 and IFITM2 also appeared to somewhat reduce the level of multiply-spliced transcripts (Fig. 5G), though the effect did not reach statistical significance, but was nonetheless coupled with a clear accumulation of ribosome-free multiply-spliced transcripts in low concentration sucrose fraction (Fig. 5G - fraction 6) relative to vector control, similar to other viral transcript classes. These data were consistent with our analysis of viral production (Fig. 1) wherein IFITM1 and IFITM2 expression lead to a more potent block in viral production than for IFITM3. Thus IFITM proteins inhibit translation of HIV-1 transcripts by leading to their specific exclusion from polysomes, resulting in reduced levels viral proteins and reduced viral output.

**HIV-1 RNA is a determinant of IFITM-mediated restriction of protein synthesis.** To better understand how IFITM proteins help suppressing viral translation, we explored the possibility that they may be involved

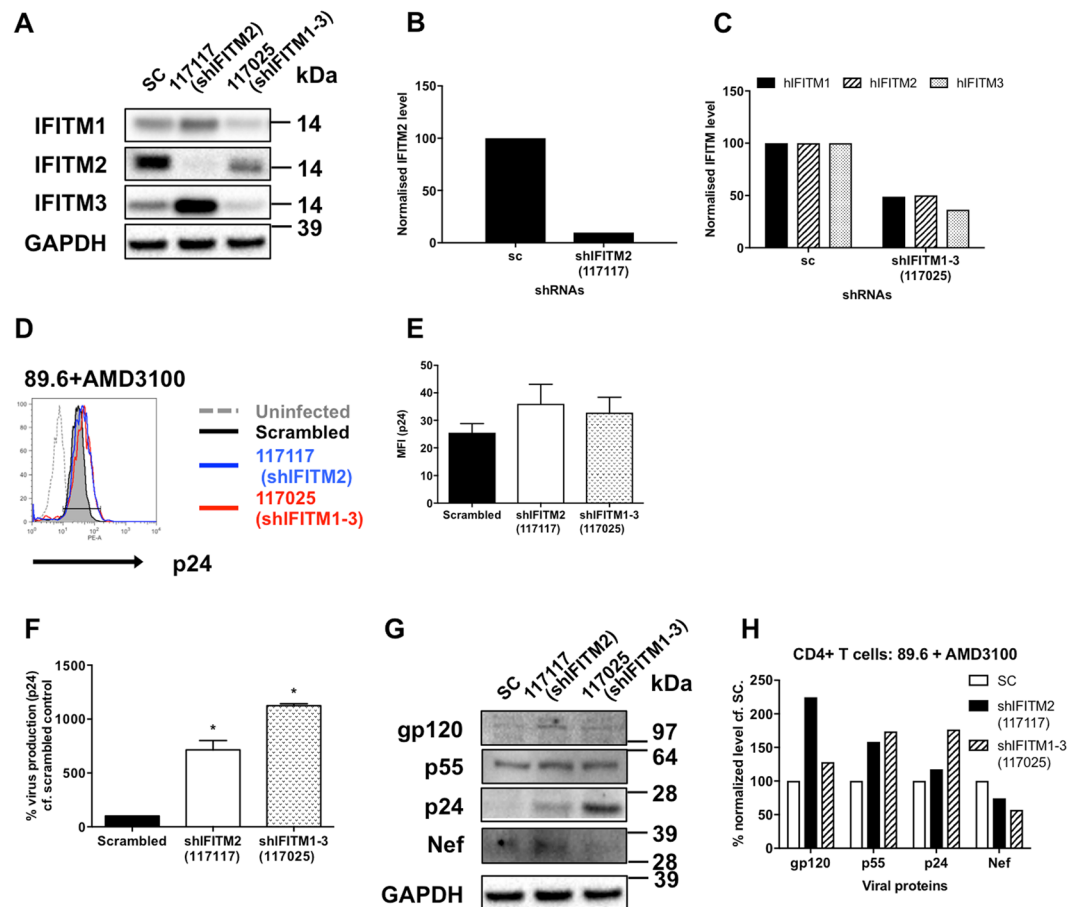


**Figure 4.** Knockdown of IFITMs rescues HIV-1 output and viral protein production in primary human T cells. Activated human CD4<sup>+</sup> T cells were transduced with lentivirus expressing the indicated shRNAs against IFITMs or scrambled sequence (sc) for 48 hours. (A) Level of IFITM expression was analyzed by immunoblotting and (B) densitometry; data was normalized to GAPDH and scrambled control. Cells were then infected with HIV-1 89.6 with equivalent p24 concentrations. Cells were pre-treated with AMD3100 for 2 hours prior to infection and throughout. Viral proteins in infected cells was analyzed by immunoblotting. Immediately after infection (3 h post-infection), cells were treated with trypsin and washed with PBS before intracellular staining of p24 and flow cytometry to measure virus uptake. Intracellular levels of p24 and median fluorescence intensity are shown in (D) representative histograms and (E) summary bar chart. (F) Level of virus production was measured by p24 ELISA 72 hours post-infection and normalized. Levels of viral proteins in infected cells from one of the blood donors were shown by (G) immunoblotting and (H) densitometry. Data show mean + S.E.M. of 2 blood donors. Differences were assessed with Student's t-test and \*indicates  $p < 0.05$ .

in a process that is able to distinguish viral RNA from cellular RNA. To address this, we measured the level of unspliced viral RNA transcripts in the polysome fraction of HEK293T cells transfected with a codon-optimized vector for HIV-1 NL4-3 Gag only<sup>33</sup> in conjunction with IFITM-expression vectors. Codon-optimization changes the codon bias of the construct towards human and therefore also alters the secondary structures of viral RNA. Changing codon bias thus renders HIV-1 unspliced and singly-spliced transcript expression independent of the HIV Rev responsive element (RRE), a *cis* acting RNA structure necessary for transcript nuclear export<sup>34</sup>. Codon optimization of *gag* rescued the level of unspliced HIV-1 transcripts in polysomes during IFITM expression, nor was there an accumulation of transcripts in low sucrose fractions as was seen with wild type NL4-3 (fraction 7 in Fig. 6A compared to fractions 6 in Fig. 5E–G). As a result, the level of extracellular p24 production from cells expressing IFITM1 and IFITM2 was not only rescued but enhanced, and the production of the *gag* products p55 and p24 was also restored in comparison to wild type NL4-3 (Fig. 6B, C, F). Notably p24 protein production was only partially rescued, but p55 was entirely rescued (Fig. 6F). Contrasting data for full length pNL4-3 DNA show clear losses of viral production and protein expression in similar experiments (Fig. 6D–F).

We then sought to identify specific RNA features that may render HIV-1 susceptible to an IFITM-driven translational block. As our findings of transfected HEK293T cells showed that unspliced and singly-spliced viral transcripts are more readily excluded from polysomes by IFITM proteins than multiply-spliced transcripts in those cells (Fig. 5), we reasoned that RRE, which is present in only unspliced and singly-spliced transcripts may be somehow recognized during IFITM protein expression leading to translational inhibition. To address this, we exploited constructs in which singly-spliced and unspliced transcripts had been rendered RRE and Rev independent via the introduction of the Mason Pfizer Monkey Virus (MPMV) constitutive transport element (CTE)<sup>35</sup>.

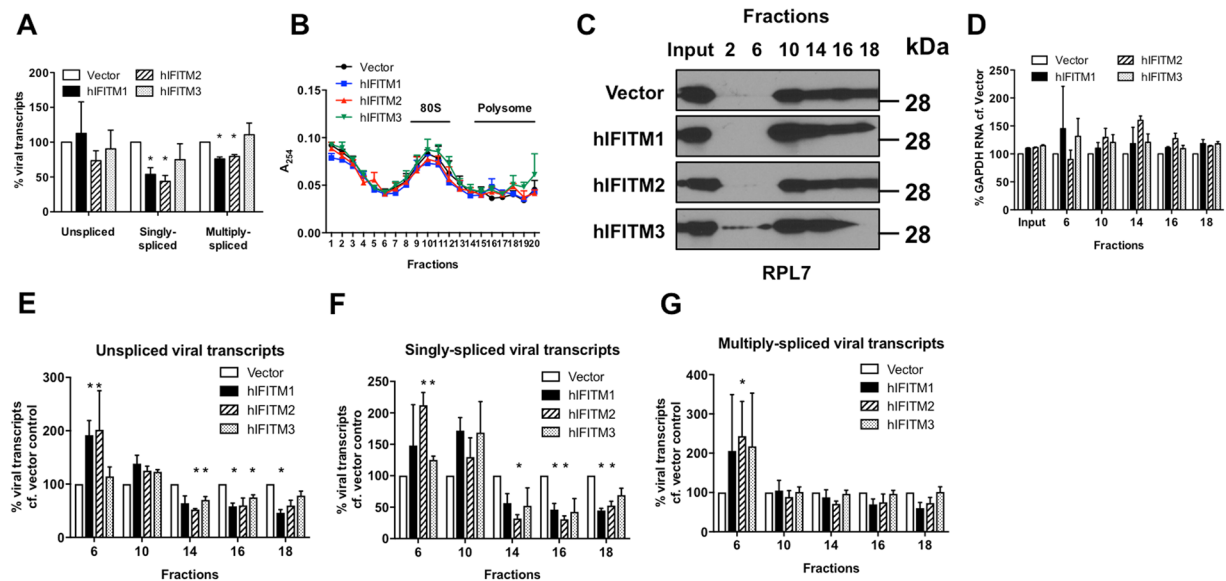


**Figure 5.** IFITM proteins inhibit HIV-1 protein synthesis. (A) Level of viral transcripts in HEK293T cells transfected with HIV-1 NL4-3 and IFITM DNA was measured by qPCR 48 hours post-transfection and the data normalized. (B) Level of RNA in sucrose gradient fractions of HEK293T cells transfected with proviral HIV-1 NL4-3 DNA and expression vectors for IFITMs (or vector alone) was measured by absorbance at 254 nm. (C) Level of ribosomal protein L7 was analyzed by immunoblotting to identify fractions enriched for polysomes. (D) Level of GAPDH RNA in IFITM-expressing cells was normalized to vector control in the indicated sucrose gradient fractions. Level of (E) unspliced, (F) singly-spliced and (G) multiply-spliced viral transcripts in the indicated sucrose gradient fractions in (B) was analyzed by qPCR then normalized with the levels of GAPDH RNA and input RNA. Data shows mean + SEM of 3 independent experiments. Differences were assessed by Student's t-test and \*denotes  $p < 0.05$  compared to vector control.

A modification which allows all transcripts to be exported from the nucleus by the cellular TAP/NXT1 pathway, rather than RRE bearing Rev-dependent transcripts exporting via the CRM1 pathway<sup>36</sup>. We found that CTE dependent Rev independent virus was still inhibited by IFITM proteins (Figure S5), demonstrating at least that nuclear export pathway does not affect the virus production inhibition seen with IFITM proteins. Further introduction of the RRE into CTE bearing constructs did also not augment the restriction.

Overall, these data suggest that the restriction of translation by IFITMs occurs at the RNA level, though it is not clear that the RRE plays a significant role in susceptibility, despite that RRE bearing transcripts are more affected in translation. Therefore some other distinguishing feature of viral transcripts or translation determines their susceptibility to IFITM proteins.

**HIV Nef can help overcome IFITM-mediated restriction of virus production.** Under the selective pressure of cellular restriction factors, retroviruses have evolved to counteract surveillance and restriction by host antiviral factors (reviewed in<sup>1</sup>). We therefore sought to investigate if HIV is able to counteract the restriction of viral production by IFITM proteins. We reasoned that HIV-1 Nef may influence this process. IFITMs are membrane proteins and lentiviral Nef regulates the trafficking of many membrane proteins such as CD4, MHC-I and tetherin to aid immune evasion and viral replication<sup>37–39</sup>. Further, the expression of a dominant negative form of HIV-1 Nef<sup>40</sup>, or *nef* deletion has previously been linked to deficits in viral production<sup>41</sup>.

We therefore measured the level of virus production in HEK293T cells transfected with expression vectors of IFITMs with wild type or *nef*-deleted HIV-1 NL4-3 proviral DNA. The level of *nef*-deleted virus produced was inhibited 18-fold by IFITM1, 21-fold by IFITM2 and 5-fold by IFITM3, suggesting a 4-fold enhancement of virus production due to HIV-1 Nef during IFITM1 and IFITM2 expression (Fig. 7A). We confirmed a significant reduction in HIV-1 Gag (p55) levels in cells producing *nef*-deleted virus while IFITMs are expressed (Fig. 7B), indicating that Nef may rescue the translational suppression driven by IFITMs. As these data were generated through transfection, they were independent of any influence of Nef upon viral entry<sup>7,8</sup>. It is also of note that exogenous IFITM levels were not reduced by HIV-1 Nef, perhaps indicating that antagonism of IFITM proteins may not occur via degradation (Fig. 7B).

We next investigated if Nef presented an advantage to viral growth in infected T-cells. We infected SupT1 cells with either wild type or *nef*-deleted NL4-3 virus by post-entry induction of IFITM expression via doxycycline (Fig. 7C). We found IFITM expression was typically very weak or absent in SupT1 cells unless induced. As *nef*-deleted virus has an inherent growth defect, we normalized the quantity of wild type and *nef*-deleted virus produced from IFITM-induced cells to vector control cells. We chose to induce IFITMs after X4-tropic HIV-1 NL4-3 entry and limit infections to a single round through the use of the CXCR4 antagonist AMD3100 after infection to mitigate the influence of IFITMs upon viral entry. In this regard, we found that *nef*-deleted virus was no more susceptible to IFITM-mediated restriction of entry than wild type virus (Figure S6A). Compared to wild



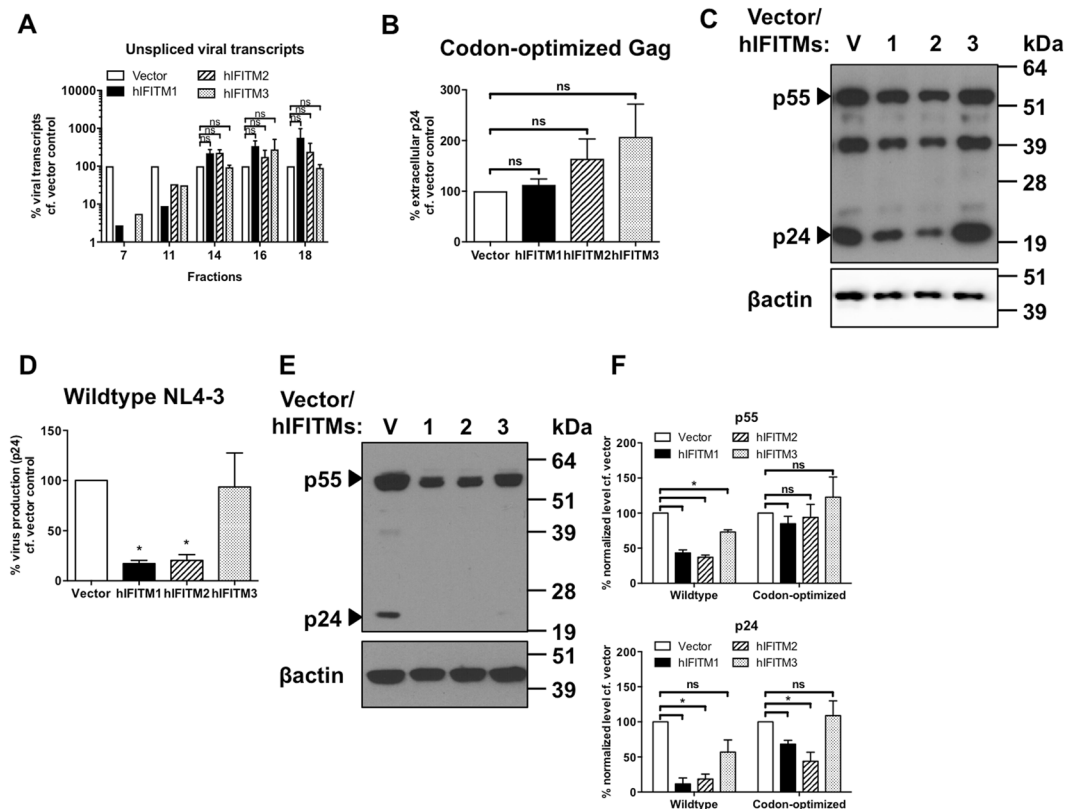


**Figure 6.** HIV-1 RNA is a determinant of IFITM-mediated inhibition of protein synthesis. (A) Normalized levels of unspliced viral transcripts (measured by qPCR) in the polysome fractions of HEK293T cells transfected with codon-optimized HIV-1 NL4-3 Gag DNA and IFITM expression vectors at 48 h post-transfection. (B) Levels of extracellular p24 in HEK293T cells transfected with codon-optimized HIV-1 Gag DNA measured by p24 ELISA 48 h post-transfection and normalized. Cellular levels of HIV-1 Gag (p55 and p24) were analyzed by (C) immunoblotting. (D) Levels of virus production in HEK293T cells transfected with 0.5  $\mu$ g wild-type HIV-1 NL4-3 proviral DNA and 0.5  $\mu$ g IFITM-expression plasmids or empty vector was measured by p24 ELISA 48 hours post-transfection and normalized. Cellular levels of HIV-1 Gag (p55 and p24) in cells transfected were analyzed by (E) immunoblotting and (F) densitometry. Data show mean + SEM of 3 independent experiments and differences were assessed by Student's t-test, \*denotes  $p < 0.05$  compared to vector control.

type virus, production of *nef*-deleted virus in infected SupT1 cells was reduced significantly during expression of all IFITMs (Fig. 7C – compare wild type graph to *nef*-deleted graph), surprisingly IFITM3 showed the greatest degree of rescue in SupT1 cells, in contrast to data for transfected 293T cells (Fig. 7A,B).

To further confirm the role of IFITM1 in suppressing virus production in T cells, we monitored the production of either wild type or *nef*-deleted HIV-1 NL4-3 virus in multiple cycle infections in a C8166 T-cell line transduced to constitutively over-express IFITM1. As IFITM1 does not typically affect the entry of CXCR4-tropic virus such as NL4-3 any difference in replication measured between wild type and *nef*-deleted virus could only arise from IFITM1-mediated effects on viral production, not cell entry<sup>16,22,23</sup>. Therefore this experiment was not pursued for IFITM2 and IFITM3, as their constitutive expression would inhibit NL4-3 virus entry and complicate interpretation. We found that in the presence of IFITM1, the growth of *nef*-deleted virus was significantly reduced relative to wild type virus (Fig. 7D). As wild type and *nef*-deleted virus data in C8166 cells were individually normalized to the same viruses in C8166 vector control cells, the differences observed are not likely due to Nef overcoming SERINC3/5 expression<sup>7,8</sup>, as these factors would be similarly present in both cell lines. Interestingly, the benefit of Nef expression in the context of IFITM1 was lost in the later stages of viral culture, when cell-to-cell infection typically predominates<sup>42</sup>. As *nef*-deleted virus was no more susceptible to IFITM-mediated restriction of entry than wild type virus (Figure S6A), these findings are only due to the influence of Nef to partially rescue virus production as seen in 293T cell transfections and SupT1 infections (Fig. 7A–C).

We then investigated if Nef from other lentiviruses was able to overcome IFITM-mediated inhibition of protein synthesis using an HIV-1 NL4-3 plasmid proviral DNA into which lentiviral *nef* alleles had been substituted<sup>43</sup>. The level of virus production for HIV-1 NL4-3 bearing other *nef* alleles during IFITM expression was generally comparable to levels for wild type NL4-3 *nef* (Fig. 7E), indicating that ability of lentiviral Nef proteins to overcome IFITM mediated restriction of virus production is common.

To further confirm the role of Nef in antagonizing IFITMs, we titrated a plasmid bearing NA7 *nef* into cells transfected with IFITM expression plasmids and *nef*-deleted NL4-3 proviral HIV-1 DNA. Nef expression *in trans* rescued viral production from IFITM-mediated inhibition in a dose dependent manner (Fig. 7F). However, we

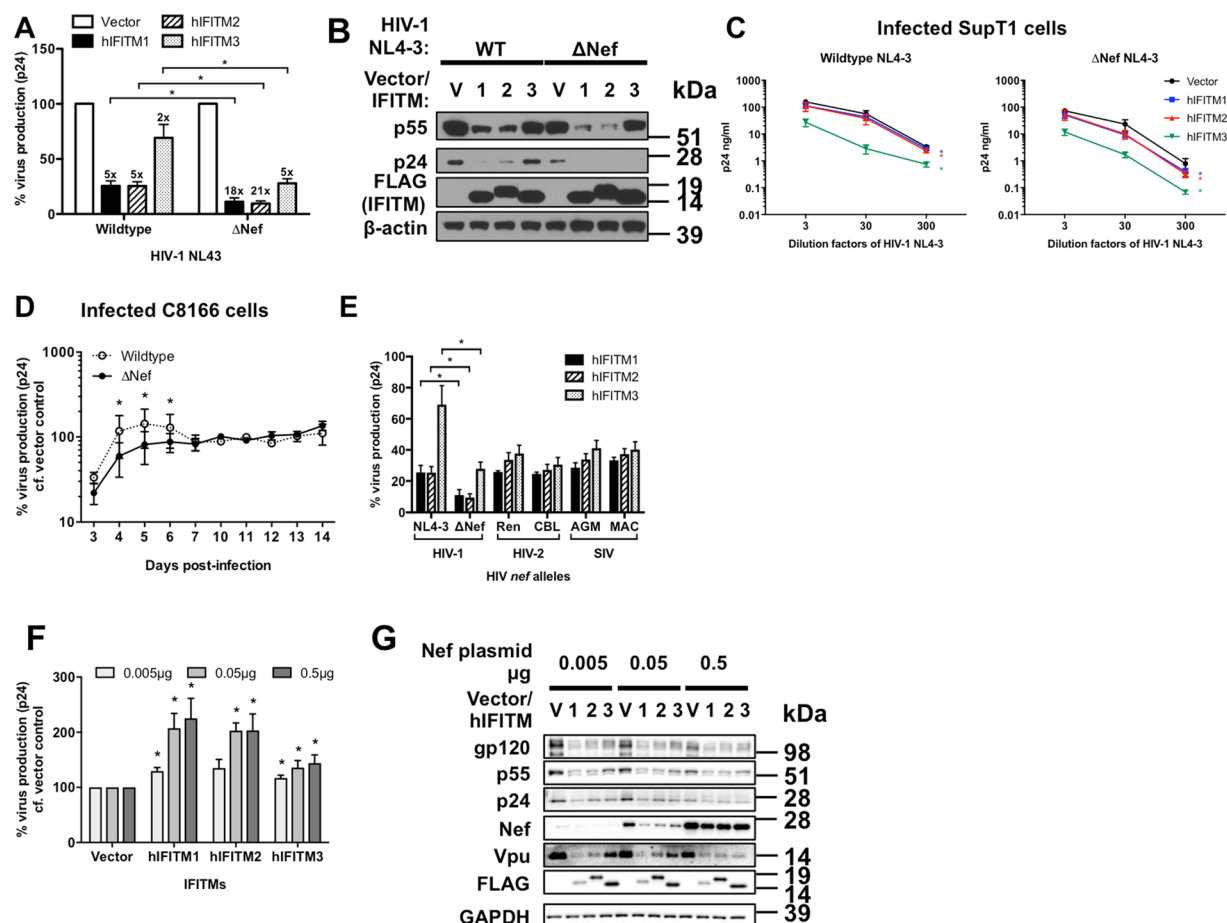


**Figure 7.** HIV Nef can help overcome IFITM-mediated restriction of protein synthesis. (A) Level of virus production in HEK293T cells transfected with 0.5 μg expression vectors for IFITMs and 0.5 μg HIV-1 NL4-3 proviral DNA with a deletion (ΔNef) was measured by p24 ELISA 48 hours post-transfection and the data normalized, fold change of virus production compared to vector control is indicated. Differences were assessed with Student's t tests. (B) Intracellular level of p55/p24 and IFITMs was measured by immunoblotting. (C) SupT1 cells were infected with the indicated dilutions of wild type or Nef-deleted (ΔNef) HIV-1 NL4-3 inoculum and then treated with 1 μg/ml doxycycline to induce IFITM expression post-entry and 5 μM AMD3100 to limit infections to a single round. Level of virus production was measured by p24 ELISA 72 hours post-infection. Differences were assessed with Two-way ANOVA and Bonferroni post-tests. (D) C8166 cells constitutively expressing either vector control or IFITM1 were infected with either wild type or Nef-deleted (ΔNef) HIV-1 NL4-3. Levels of virus production were measured by p24 ELISA at the indicated time-points post-infection and were normalized to the levels of virus produced from vector controls. Differences were assessed with Two-way ANOVA. (E) HEK293T cells were transfected with 0.5 μg expression vectors for IFITMs and 0.5 μg HIV-1 NL4-3 proviral DNA with either wildtype NL4-3 *nef* or the indicated lentiviral *nef* alleles. Virus production was measured by p24 ELISA 48 hours post-transfection and the data normalized. Differences were assessed with Student's t tests. (F) HEK293T cells were transfected with ΔNef HIV-1 NL4-3 proviral DNA, expression vectors for IFITMs and an increasing proportion of HIV-1 Nef-encoding vector versus empty vector in a fixed total quantity of 1 μg. Level of virus production was measured by p24 ELISA 48 hours post-transfection, while levels of viral proteins and IFITM-FLAG expression was analyzed by (G) immunoblotting. Differences were assessed by Student's t-test. All data show mean + SEM from 3 independent experiments and \*denotes  $p < 0.05$ .

note overexpression of Nef in cells transfected with 0.5 μg Nef-encoding plasmid resulted in an overall lower level of viral proteins compared with cells expressing lower levels of Nef. Interestingly, increased Nef levels helped restore viral production in the context of IFITM expression (Fig. 7F), this rescue was not reflected in viral protein production levels (Figs 7G and S4C), implying that the ability of Nef to rescue HIV production during IFITM expression does not occur at the level of protein synthesis. In summary, these data show that Nef can help overcome IFITM-mediated inhibition of HIV-1 production in a concentration-dependent manner. Taken together, our data demonstrate that HIV-1 Nef is able to help overcome the inhibition of viral protein production exerted by IFITM proteins and therefore enhance infection.

## Discussion

We report here that IFITM proteins restrict HIV-1 by excluding viral mRNA from polysomes thereby specifically inhibiting protein synthesis. By variously using transfection, post-entry IFITM induction, and viral co-receptor bypass strategies, we have identified a viral entry independent effect due to IFITMs that inhibits viral production. Since the discovery of the antiviral effect of IFITM proteins upon HIV-1 entry and infectivity, there have been data suggesting that there may be a distinct IFITM function directed towards HIV-1 production<sup>10,12,14,15,23–27</sup>. Despite the relative frequency of these passing observations on viral production, the underlying processes leading to loss of viral production during IFITM expression have not been explored.

We have demonstrated the breadth of the IFITM-mediated restriction of virus production, identified the viral replication process that is subverted, and determined a means by which HIV-1 may partially overcome this effect. In addition, we find that restriction of viral production by IFITM proteins is clear contributor towards the inhibition of HIV-1 production seen in cells exposed to type I interferon, and have also shown that inhibition occurs in primary CD4<sup>+</sup> T-cells at physiologically relevant levels of endogenous IFITM expression. From a mechanistic perspective we have shown that HIV-1 RNA is the target of this inhibition, though the viral determinant remains elusive. We therefore propose that inhibition of viral protein synthesis is a genuine antiviral function exerted by IFITM proteins that is distinct from previously described effects upon entry and infectivity.

Initial suggestions of a late-stage IFITM-mediated restriction have typically surrounded two common laboratory HIV-1 strains, NL4-3 and BH10<sup>10,12,14,26,27</sup>. However, for the putative anti-HIV restriction factor viperin/RSAD2, analysis demonstrated that the phenotype could not be replicated beyond the laboratory strain NL4-3<sup>44</sup>. Therefore our demonstration that IFITM proteins restrict production of multiple HIV-1, HIV-2 and SIVs implies the phenotype we observe is likely not an artefact. This is supported by our finding that African Green Monkey IFITM1 can exert a similar antiviral effect upon HIV-1 production as occurs with human IFITM1.

The general mechanism of restriction we outline is specific exclusion of HIV-1 mRNA from polysomes during IFITM expression. In HEK293T cells the effect principally occurs with IFITM1 and IFITM2, but less so for IFITM3, and was generally consistent throughout our analysis. Yet inducible expression of IFITM3 in SupT1 cells showed an equivalent antiviral effect to IFITM1 and IFITM2 though, and this was also linked to viral protein loss and was independent of IFITM-driven effects on viral entry. We consider that the same translational blocks measured in polysome analysis of HEK293T cells drive the result seen in SupT1 cells and primary CD4<sup>+</sup> T-cells. Indeed, we considered it very likely cell type specific differences would occur, as IFITM localization and thus antiviral activity are governed by both ubiquitination and palmitoylation<sup>25,45</sup>. Reasonably the degree to which IFITM-driven viral entry inhibition or viral translation inhibition occurs in particular cells is then influenced by the activity of these pathways, which are known to commonly vary. Equally, other cell specific factors influencing viral transcription (such as NFκB translocation) might also account for variation in antiviral activity between cell lines, as higher virus transcriptional activity may overcome inhibition. However, it is important to note that we were able to clearly confirm the inhibition of viral production in primary human CD4<sup>+</sup> T-cells by IFITM2 and IFITM1-3, demonstrating that inhibition of viral production by IFITMs occurs in HIV-1 target cells at physiologically relevant levels of endogenously expressed IFITM proteins.

Why IFITM1 and IFITM2 should act so similarly in many of our experiments in 293T cells and differently to IFITM3, when IFITM2 and IFITM3 have highly more closely related amino acid sequences than to IFITM1 is not yet clear<sup>10,19,46,47</sup>. IFITM-mediated antiviral effects upon viral entry are principally determined by cellular localization, and we anticipate the inhibition of protein synthesis we studied here to be similar<sup>45,46,48</sup>. Notably, IFITM2 and IFITM3 typically show distinct cellular localization which may be important in influencing their ability to inhibit virus production despite their high sequence similarity.

The exclusion of viral transcripts from polysomes seemed to mainly affect unspliced and singly-spliced transcripts. Yet despite a lack of significance, there was consistent but weaker loss of multiply spliced transcripts from polysome fractions, coupled with multiply-spliced transcript enrichment in low sucrose fractions. This is perhaps indicative of some degree of multiply-spliced transcript translational blockage that explains the loss of Nef protein seen throughout our experiments.

We saw no change in total unspliced mRNA levels in IFITM expressing cells yet there was modest depletion of singly-spliced and multiply-spliced mRNA during IFITM1 and IFITM2 expression. Though this overall depletion of total viral mRNA levels may partially account for some loss of Vpu and Nef production, polysome analysis additionally demonstrated clear exclusion of these transcript classes from translation. Why these overall mRNA levels should be reduced is of interest. One possibility is a transcriptional inhibition or pre-translational degradation, but degradation of mRNAs that have been inhibited in translation is thought to be common<sup>49</sup>. For example, the antiviral protein ZAP, which degrades retroviral mRNA has also been shown to stall translation prior to mRNA degradation, illustrating the fluid link between translational stalling and mRNA stability<sup>50,51</sup>.

Susceptibility to inhibition occurred at the level of viral mRNA and we so sought to identify a viral RNA susceptibility determinant. Our data showing *gag* codon optimization relieves the late-stage IFITM inhibition of HIV-1 supports similar findings<sup>27</sup>. Singly-spliced and unspliced transcripts that bear the RRE were typically most affected by IFITMs proteins in our analyses. Yet investigation of proviral constructs in which the RRE was substituted for the CTE element were inconclusive, making it difficult to reconcile a role for the RRE in determining inhibition, despite the appealing observation that RRE bearing transcripts are typically most affected. Notably, RRE bearing transcripts also have a non-human codon bias and surrounding splice sites that may prove to influence restriction<sup>52–55</sup>. As such further analysis to identify any HIV-1 RNA determinant of inhibition will then be of much value, though currently our further attempts to identify the viral RNA determinant have been unsuccessful. A recent study demonstrated that viral RNA CG dinucleotide frequency drives ZAP-mediated viral restriction rather than a specific RNA structural determinant, thus the determinant for IFITM-mediated restriction of protein synthesis may be similarly obscure<sup>56</sup>. However, we were able to exclude the broader possibility of general translational arrest via IFITM expression. Other aspects of the mechanism remain elusive also. IFITMs

have no reported RNA binding domain and so would require either an RNA-binding partner to directly achieve inhibition, or would need to be involved in a pathway that could influence translation in this manner.

IFITMs are cofactors in direct inhibition of viral RNA translation, it is not yet clear how a membrane protein can affect both soluble protein translation and membrane protein translation, this may ultimately depend on the absolute strictness of translational site partitioning, a concept which is under renewed debate<sup>57</sup>. Further, typically a proportion of IFITM proteins in cells are not palmitoylated and show less distinct membrane localization, conceivably this fraction may be important in influencing translation<sup>45</sup>. One unexplored possibility is that the capacity of IFITM proteins to disrupt membrane fluidity or other membrane physical characteristics to inhibition viral-cell membrane fusion<sup>17,58</sup> on the cell surface and in endosomal compartments similarly affects rough endoplasmic reticulum membranes, leading to a disruption of membrane bound translational complexes. Though how such a process could be specific to virus translation is unclear.

We demonstrate that the lentiviral protein Nef can help overcome the late-stage inhibition of viral production exerted by IFITM proteins. Though notably this rescue is not complete. Our data may help explain accounts of a Nef driven enhancement of HIV-1 production<sup>40,41</sup>. The ability to overcome IFITM-mediated inhibition of virus production was apparent with all HIV-1, HIV-2 and SIV *nef* alleles tested.

Though the underlying mechanism of ability of Nef to counter IFITMs is unclear, we saw no degradation of IFITMs in the context of viral protein expression. One possible explanation may be re-trafficking, wherein Nef acts as an adaptor protein to direct IFITMs away from their site of action on translation. This fits well with the sensitivity of IFITM-mediated antiviral function to changes in IFITM localization<sup>45,46,48</sup>, but also fits with the ability of Nef to redirect a multitude of membrane proteins from their site of action<sup>38,39,59,60</sup>. This may be consistent with our observation that Nef rescues virus particle production in supernatants during IFITM expression, but does not rescue viral protein production.

We also found that, in multiple cycle infections, the benefit of Nef expression was only seen early in culture but was latterly lost. Cell-free infection is prevalent in the early stages of culture, but infection shifts towards a cell-to-cell mode in later stages<sup>42</sup>. It has been proposed that this represents a means of escape from immune factors in HIV-1; as the high efficiency, high multiplicity of infection associated with cell-to-cell transmission can overcome restriction<sup>61,62</sup>. For example, with the antiviral restriction factor tetherin, antiviral effect is either severely weakened or absent during cell-to-cell transmission of HIV-1<sup>31,63,64</sup>.

Thus we conclude that IFITMs are antiviral factors that can target HIV-1 translation. For retroviruses this seems to be a recurring weak point in replication strategy that the innate immune system has frequently evolved to target. For example, PKR senses viral double stranded RNA and halts translation<sup>65</sup>, while Schlaffen 11 inhibits viral protein production by disrupting tRNA synthesis<sup>66</sup>, and finally the protein ZAP which induces viral mRNA degradation also stalls viral translation<sup>51</sup>.

The model we put forward wherein IFITM expression specifically disrupts viral mRNA translation may be applicable to other targets. Conceptually, other self and non-self RNAs may be affected also. It is then of interest that a recent report found that LINE-1 retrotransposon mobility could be inhibited by IFITM1 expression<sup>67</sup>, which for a retrotransposon cannot of course arise from viral entry effects. Future characterization will therefore identify the viral RNA determinant of susceptibility, and the breadth of antiviral and RNA regulatory response driven by IFITM proteins.

## Methods

**Plasmids.** Human pQCXIP IFITM1–3 plasmids bearing an N-terminal FLAG were previously described<sup>58</sup>. The viral construct pBR4-3-eGFP-Nef, encoding for wild type HIV-1 NL4-3, pBR4-3-eGFPΔNef, HIV-1 NA7, HIV-1 NL4-3 plasmids carrying *nef* alleles of HIV-2 Ren or CBL and SIV AGM or MAC strains - all described in<sup>43</sup> - are kind gifts of Professor Frank Kirchhoff (University of Ulm). HIV-2 MCR and MCN plasmids<sup>68</sup> are kind gifts of Professor Áine McKnight (Queen Mary University of London). pSIV<sub>agm</sub>Tan-1, pSIV<sub>cpz</sub>Tan1.910 and pSIV<sub>mac</sub>1A11 are from NIH AIDS Reagent Program. Codon-optimized HIV-1 NL4-3 is encoded by pCNC-SYNGP<sup>33</sup> (Oxford BioMedica). Plasmids pCTEΔEnvΔRevΔRRE and pCTEΔEnvΔRev<sup>35</sup> are kind gifts of Professor Paul Bieniasz (Rockefeller University). Plasmid HA-FLAG-GFP was a kind gift from Dr Maxine Linial (Fred Hutchinson Cancer Research Center), while GFP was also expressed from pC3-GFP (Clontech).

**Antibodies, cells and antiviral compounds.** The following antibodies were used to detect IFITMs: human IFITM1 (clone 5B5E2, Proteintech), IFITM2 (clone 3D5F7, Proteintech) and human IFITM3 (clone EPR5242, Novus Biologicals). Anti-Flag (clone M2, Sigma) was used to detect FLAG-tagged IFITMs, Rev and GFP. Anti-HIV1 Nef (clone 3F2, ThermoFisher), rabbit polyclonal anti-Vpu (Abcam) and rabbit polyclonal anti-HIV1 Gag (Abcam) were used to detect viral proteins. As loading control, β-actin (clone AC74, Sigma) and GAPDH (Abcam) antibodies were used. Secondary antibodies were horseradish peroxidase conjugated goat anti-rabbit/mouse IgG. TZM-bl cells expressing shRNAs targeting IFITMs were previously described<sup>28</sup>, as were SupT1 cells inducible for IFITM expression<sup>10</sup>. Human Embryonic Kidney (HEK) epithelial 293T cells (HEK293T), C8166 cells, TZM-bl cells, and SupT1 cells were maintained in standard conditions, and were all originally procured from the NIH AIDS Reagents Program. Primary monocytes and CD4<sup>+</sup> T cells were isolated from leukocyte cones (NHS Blood Transfusion service, St. George's Hospital, London) using the human CD14<sup>+</sup> and CD4<sup>+</sup> T cell isolation kits, respectively, according to manufacturer instruction (Miltenyi Biotec). 0.5 × 10<sup>6</sup>/ml CD14<sup>+</sup> monocytes were differentiated into macrophages with 100 ng/ml GM-CSF (Peprotech) at 2–3 days interval until day 7. CD4<sup>+</sup> T cells were activated at 1 × 10<sup>6</sup>/ml with T cell activator CD3/CD28 Dynabeads (ThermoFisher), at a bead-to-cell-ratio of 1:1, in complete medium (RPMI 1640 medium supplemented with 10% heat-inactivated fetal bovine serum, 2mM L-glutamine, 100U/ml streptomycin, 100U/ml penicillin, all from ThermoFisher) and 30U/ml IL-2 (Peprotech) for 48 hours. AMD3100 and Maraviroc were obtained via the NIBSC AIDS Reagent Program.



**Transfections.** HEK293T cells were plated at  $2 \times 10^4/\text{cm}^2$  in 48-well plates (for measurements of virus production), 6-well plates (for measurements of whole cell viral transcripts by qPCR), 10 cm dishes (for virus production, polysome analysis and immunoprecipitation, all from Nunc), 48 hours before transfection. Plasmid DNA (total quantity of  $1 \mu\text{g}/\text{well}$  in 48-well plates,  $3 \mu\text{g}/\text{well}$  in 6-well plates and  $5 \mu\text{g}/\text{well}$  in 10 cm dishes) was diluted in OptiMEM (ThermoFisher) at 10% volume of total cell culture medium. Equal quantity of different plasmid DNA was added in co-transfection. Linear polyethylenimine (L-PEI) was added at a w/w ratio of 5:1 into the diluted DNA. The transfection mixture was incubated at room temperature for 10 minutes before added to cells.

For transfections in 96 well plates for GFP analysis,  $2 \times 10^4$  HEK293T cells were seeded into 96 well plates containing  $0.3 \mu\text{l}$  Lipofectamine 2000 (ThermoFisher) diluted in OptiMEM (ThermoFisher) with  $100 \text{ ng}$  total plasmid DNA per well.

For siRNA transfection experiments, HEK293T cells were plated at  $1 \times 10^4/\text{cm}^2$  24 hours prior to transfection in 48-well plates. siRNAs at a final concentration of  $100 \text{ nM}$  was added to a total of  $100 \mu\text{l}$  OptiMEM, incubated for 5 minutes at room temperature and then  $1 \mu\text{l}$  DharmaFECT 1 (Dharmacon) was added to diluted DNA. siRNA-transfection mix was incubated for 20 minutes at room temperature and then added to cells. Expression vectors of IFITMs and HIV-1 proviral DNA were transfected then 48 hours post-transfection.

TZM-bl cells were plated at  $6 \times 10^4/\text{cm}^2$  in 48-well plates 24 hours before transfection. In a 48-well format,  $1 \mu\text{g}/\text{well}$  plasmid DNA and  $6 \mu\text{l}$  Lipofectamine 2000 (ThermoFisher) were diluted in OptiMEM, incubated for 10 minutes at room temperature and then added to cells. Medium was replaced with medium containing  $5 \mu\text{M}$  AMD3100 and  $100 \text{ IU}/\text{ml}$  IFN- $\beta$  (Peprotech) 4 hours post-transfection.

**Intracellular staining and flow cytometry.** IFITM expression in IFN $\beta$ -treated human MDMs,  $\text{CD4}^+$  T cells, transfected HEK293T cells and doxycycline-treated SupT1 cells was detected by fixing cells in 4% (w/v) paraformaldehyde (Sigma) in PBS for 15 minutes at room temperature, followed by permeabilization in 0.2% (v/v) Triton X-100 (Sigma) for 20 minutes at room temperature. Cells were then blocked in 5% BSA in PBS for 1 hour at room temperature followed by incubation with  $1 \mu\text{g}/\text{ml}$  IFITM-specific monoclonal antibodies diluted in staining buffer (2% BSA/0.1% Triton X-100/PBS) overnight at  $4^\circ\text{C}$ . Cells were washed 3 times with 2% BSA in PBS and labelled with secondary antibodies, human IFITM1, 2 and 3 antibodies were detected by  $0.5 \mu\text{g}/\text{ml}$  goat anti-mouse IgG2a Alexa Fluor 647, goat anti-mouse IgG1 Alexa Fluor 488 and goat anti-rabbit Alexa Fluor 350, respectively, in staining buffer for 1 hour at room temperature. Labelled cells were washed 3 times in 2% BSA in PBS and analyzed on LSR II flow cytometer (BD). Data was analyzed on FlowJo (BD).

**Infection.** Virus production and infections were performed in a BSL3 laboratory in accordance with local health and safety regulations. HIV-1 virus was produced from transfected HEK293T cells. SupT1 cells were spinoculated with the indicated concentrations of inoculum for 2 hours at  $37^\circ\text{C}$  at  $1000 \times g$  in 96-well U-bottom plates (Nunc) followed by incubation at  $37^\circ\text{C}$  for 1 hour. Infected cells were then washed 3 times with phosphate-buffered saline (PBS, Sigma) and re-suspended in medium with  $1 \mu\text{g}/\text{ml}$  doxycycline (Sigma) and  $5 \mu\text{M}$  AMD3100. C8166 cells were infected with the same protocol without AMD3100. Supernatant was harvested at the indicated time-points after centrifugation at  $500 \times g$  for 5 minutes at room temperature.

**Transduction and infection of primary human  $\text{CD4}^+$  T cells.** In the presence of CD3/CD28 T-cell activator beads,  $5 \times 10^5/\text{ml}$  activated  $\text{CD4}^+$  T cells were transduced with IFITM-targeting or scrambled shRNA lentivirus with p24 at  $100 \text{ ng}/\text{ml}$  for 2 hours at  $1000 \times g$ ,  $37^\circ\text{C}$  and then for 1 hour incubation. Infected cells were washed three times with PBS, re-suspended in complete medium with  $30 \text{ U}/\text{ml}$  IL-2 and then incubated at  $37^\circ\text{C}$  for 48 hours. Prior to HIV infection, T cell activator beads were removed from transduced  $\text{CD4}^+$  T cells. Transduced  $\text{CD4}^+$  T cells were then incubated with medium alone,  $5 \mu\text{M}$  Maraviroc or  $5 \mu\text{M}$  AMD3100 for 2 hours at  $37^\circ\text{C}$ . Untreated cells and drug-treated cells were then infected with  $100 \text{ ng}/\text{ml}$  p24 of NL4-3 or 89.6 virus, respectively, at  $37^\circ\text{C}$ ,  $1000 \times g$  for 2 hours and then incubated for 1 hour. Infected cells were then washed three times with PBS and re-suspended in complete medium containing  $30 \text{ U}/\text{ml}$  IL-2,  $5 \mu\text{M}$  Maraviroc and  $5 \mu\text{M}$  AMD3100. Aliquots of infected cells were treated with 0.25% Trypsin/EDTA (ThermoFisher) for 15 minutes at  $37^\circ\text{C}$ , washed three times with PBS, fixed in 2% paraformaldehyde, permeabilized in 0.2% Triton X-100/PBS and stained with RD-1 conjugated monoclonal mouse anti-HIV-1-p24 (clone KC57, Beckman Coulter) for flow cytometry analysis of internalized virus. Level of viral output in supernatant was measured by p24 ELISA 72 hours post-infection.

**p24 ELISA.** ELISA plates (Nunc) were pre-coated with  $5 \mu\text{g}/\text{ml}$  sheep anti-HIV-1 p24 antibody (Aalto Bio Reagents) at  $4^\circ\text{C}$  overnight. Supernatant of transfected HEK293T, TZM-bl cells or infected cells was treated with 1% Empigen BB (Sigma) for 30 minutes at  $56^\circ\text{C}$ , then plated at 1:10 dilution in Tris-buffered saline (TBS) on anti-p24-coated plates and incubated for 3 hours at room temperature. Alkaline phosphatase-conjugated mouse anti-HIV-1 p24 monoclonal antibody (Aalto Bio Reagents) diluted in 20% sheep serum, 0.05% v/v Tween-20, TBS (all from Sigma) was then added and incubated for 1 hour at room temperature. Plates were washed 4 times with 0.01% v/v Tween-20 in PBS and twice with ELISA Light washing buffer (ThermoFisher). CSPD substrate with Sapphire II enhancer (ThermoFisher) was added and incubated for 30 minutes at room temperature before chemiluminescence was read by a plate reader.

**Reverse transcriptase (RT) activity, luciferase activity assays, and GFP plate assays.** Colorimetric reverse transcriptase activity assay kit (Roche) was used to determine reverse transcriptase activity of HIV-1, HIV-2 and SIV in supernatants of transfected HEK293T cells. Manufacturer instructions was followed except that supernatant was first treated directly with lysis buffer ( $50 \text{ mM}$  Tris pH7.8,  $80 \text{ mM}$  potassium chloride,  $2.5 \text{ mM}$  DTT,  $750 \mu\text{M}$  EDTA and 0.5% Triton X-100, all from Sigma) for 30 minutes at room temperature and then incubated in streptavidin-coated microplates for 15 hours at  $37^\circ\text{C}$ .



Luciferase activity of infected TZM/bl cells was analyzed with Bright-Glo luciferase activity kit following manufacturer instructions (Promega). GFP expression levels in transfected cells were determined by measuring the fluorescence intensity using POLARstar plate reader (BMG Labtech) 24, 48 and 72 hours after transfection.

**Polysome profiling.** Polysome analysis was performed with both manual fractionation and RNA analysis<sup>69</sup>. Transfected HEK293T cells were incubated with 100 µg/ml cycloheximide (Sigma) for 15 minutes for 37 °C and then washed with ice-cold PBS with 100 µg/ml cycloheximide. Cells were then lysed in polysome buffer, 10 mM Tris pH8, 140 mM NaCl, 1.5 mM MgCl<sub>2</sub>, 0.5% v/v NP40, 100 µg/ml cycloheximide, protease inhibitor cocktail (all from Sigma) and 800U/ml RNase OUT (ThermoFisher), for 10 minutes on ice. Cell lysate was centrifuged at 10,000 × g for 1 minute at 4 °C and supernatant was then adjusted to 200 µg/ml cycloheximide and 700 µg/ml heparin (Sigma). Following centrifugation at 12,000 × g for 10 minutes at 4 °C, an aliquot of supernatant was taken as input and the rest was layered onto a 10% to 50% sucrose gradient prepared using polysomal buffer. Gradients were then ultracentrifuged at 300,000 × g for 16 hours at 4 °C (Sorvall). After centrifugation, 20 550 µl fractions were collected from the top of the gradients for immunoblotting and quantitative PCR analyses. Level of RNA in fractions was measured by absorbance at 254 nm (Nanodrop) and RNA was precipitated with 5x volume of absolute ethanol (Sigma) overnight at −20 °C.

**Quantitative PCR.** Total RNA of transfected HEK293T cells and precipitated RNA from polysome profiling fractions were purified with RNeasy mini kit and on-column DNA digestion with RNase-free DNase kit (both from Qiagen) following manufacturer instructions. 3 ng of total RNA per sample was analyzed with Superscript III Platinum One-Step qRT-PCR kit with ROX (for unspliced and multiply spliced viral transcripts, ThermoFisher) or QuantiTect SYBR Green PCR kit (for singly-spliced viral transcript, Qiagen) and ABI 7500 Real Time PCR system (Applied Biosystems). Cycling conditions were 50 °C C for 15 minutes, 95 °C C for 8 minutes, then cycling of 95 °C for 15 s and 60 °C for 30 s. Reactions carried out in the absence of reverse transcriptase (Platinum Taq only) confirmed the absence of DNA contamination. The samples were quantified against cloned standards.

Primers used to amplify unspliced (Forward, 5'-CCGTCTGTTGTGTGACTCTGG-3', reverse, 5'-GAGTCTGCGTCGAGAGATCT-3'), multiply-spliced (Forward, 5'-CAGACTCATCAAGCTTCTCTATCAA-3', reverse, 5'-CTATTCCTTCGGGCCTGTC-3') and singly-spliced (Forward, 5'-TAATCGGCCGAACAGGGA CTTGAAAGCGAAAG-3', reverse, 5'-CCCATCTCCACAAGTGCTGATACTTC-3') viral transcripts are described in<sup>70,71</sup>, and<sup>72</sup>, respectively. Oligonucleotide probes are labelled with 5'-FAM and 3'-TAMRA, (unspliced, 5'-TCTAGCAGTGGCGCCCGAACAGG-3' and multiply-spliced, 5'-AACCCACCTCCCAATCCCGAGG-3', all from ThermoFisher). Cellular GAPDH (glyceraldehyde-3-phosphate dehydrogenase) mRNA was additionally amplified as a loading control with primers (Forward, 5'-AGGTCTGGAGTCAACGG ATTTGG-3', reverse, 5'-GATGGCAACAATATCCACTTTACCA-3') and probe (5'-TCTTATTGGGCGCCTGGTCAC-3', as described in<sup>71</sup>).

**Immunoblotting.** Cells were washed once with PBS and then lysed in radioimmunoprecipitation buffer (RIPA, containing 20 mM Tris pH7.5, 150 mM NaCl, 1 mM EDTA, 1 mM EGTA, 1% NP40, 1% sodium deoxycholate, 250 µM sodium pyrophosphate, 1 mM β-glycerophosphate, 1 mM sodium vanadate and protease inhibitor cocktail, all from Sigma) for 30 minutes at 4 °C. Lysate was then centrifuged for 10,000 × g for 10 minutes at 4 °C. Protein concentration of supernatant was determined by bicinchoninic acid (BCA) assay (ThermoFisher). 10 µg of protein per sample was analyzed by immunoblotting, developed with ECL Prime reagents (GE Healthcare Life Sciences) and captured on CL-XPosure films (ThermoFisher) or ChemiDoc MP system (Bio-Rad). Intensity of immunobands was analyzed by ImageJ (on X-ray films) or ImageLab (Bio-Rad).

**Statistical analysis.** Levels of viral output in p24 ELISA and RT assay were normalized to vector-transfected or scrambled shRNA-transduced control and expressed as the level of virus production unless otherwise indicated. Statistical analysis was performed with Graphpad Prism 5. Data shows mean + standard error of mean from a minimum of 3 independent experiments.

## References

- Malim, M. H. & Bieniasz, P. D. HIV Restriction Factors and Mechanisms of Evasion. *Cold Spring Harb Perspect Med* **2**, a006940 (2012).
- Simon, V., Bloch, N. & Landau, N. R. Intrinsic host restrictions to HIV-1 and mechanisms of viral escape. *Cell* **163**, 546–553 (2015).
- Kluge, S. F., Sauter, D. & Kirchhoff, F. SnapShot: Antiviral Restriction Factors. *Cell* **163**, 774–774.e1 (2015).
- Liu, L. *et al.* A whole genome screen for HIV restriction factors. *Retrovirology* **8**, 94 (2011).
- Kane, M. *et al.* MX2 is an interferon-induced inhibitor of HIV-1 infection. *Nature* **502**, 563–566 (2013).
- Goujon, C. *et al.* Human MX2 is an interferon-induced post-entry inhibitor of HIV-1 infection. *Nature* **502**, 559–562 (2013).
- Rosa, A. *et al.* HIV-1 Nef promotes infection by excluding SERINC5 from virion incorporation. *Nature* **526**, 212–217 (2015).
- Usami, Y., Wu, Y. & Göttlinger, H. G. SERINC3 and SERINC5 restrict HIV-1 infectivity and are counteracted by Nef. *Nature* **526**, 218–223 (2015).
- Brass, A. L. *et al.* The IFITM proteins mediate cellular resistance to influenza A H1N1 virus, West Nile virus, and dengue virus. *Cell* **139**, 1243–1254 (2009).
- Lu, J. *et al.* The IFITM proteins inhibit HIV-1 infection. *J. Virol.* **85**, 2126–2137 (2011).
- Schoggins, J. W. *et al.* A diverse range of gene products are effectors of the type I interferon antiviral response. *Nature* **472**, 481–485 (2011).
- Wilson, S. J. *et al.* Inhibition of HIV-1 particle assembly by 2',3'-cyclic-nucleotide 3"-phosphodiesterase. *Cell Host Microbe* **12**, 585–597 (2012).
- Bailey, C. C., Zhong, G., Huang, I.-C. & Farzan, M. IFITM-Family Proteins: The Cell's First Line of Antiviral Defense. *Annual Review of Virology* **1**, 261–283 (2014).
- Compton, A. A. *et al.* IFITM proteins incorporated into HIV-1 virions impair viral fusion and spread. *Cell Host Microbe* **16**, 736–747 (2014).

15. Tartour, K. *et al.* IFITM proteins are incorporated onto HIV-1 virion particles and negatively imprint their infectivity. *Retrovirology* **11**, 103 (2014).
16. Tartour, K. *et al.* Interference with the production of infectious viral particles and bimodal inhibition of replication are broadly conserved antiviral properties of IFITMs. *PLoS Pathog* **13**, e1006610 (2017).
17. Amini-Bavil-Olyae, S. *et al.* The Antiviral Effector IFITM3 Disrupts Intracellular Cholesterol Homeostasis to Block Viral Entry. *Cell Host Microbe* **13**, 452–464 (2013).
18. Yu, J. *et al.* IFITM Proteins Restrict HIV-1 Infection by Antagonizing the Envelope Glycoprotein. *Cell Rep* **13**, 145–156 (2015).
19. Huang, I.-C. *et al.* Distinct patterns of IFITM-mediated restriction of filoviruses, SARS coronavirus, and influenza A virus. *PLoS Pathog* **7**, e1001258 (2011).
20. Wilkins, C. *et al.* IFITM1 is a tight junction protein that inhibits hepatitis C virus entry. *Hepatology* **57**, 461–469 (2013).
21. Savidis, G. *et al.* The IFITMs Inhibit Zika Virus Replication. *Cell Rep* **15**, 2323–2330 (2016).
22. Foster, T. L. *et al.* Resistance of Transmitted Founder HIV-1 to IFITM-Mediated Restriction. *Cell Host Microbe* 1–15, <https://doi.org/10.1016/j.chom.2016.08.006> (2016).
23. Wang, Y. *et al.* The V3 Loop of HIV-1 Env Determines Viral Susceptibility to IFITM3 Impairment of Viral Infectivity. *J. Virol.* **91**, e02441–16 (2017).
24. Kane, M. *et al.* Identification of Interferon-Stimulated Genes with Antiretroviral Activity. *Cell Host Microbe* **20**, 392–405 (2016).
25. Compton, A. A. *et al.* Natural mutations in IFITM3 modulate post-translational regulation and toggle antiviral specificity. *EMBO Rep.* e201642771–15, <https://doi.org/10.15252/embr.201642771> (2016).
26. Ding, S., Pan, Q., Liu, S.-L. & Liang, C. HIV-1 mutates to evade IFITM1 restriction. *Virology* **454–455**, 11–24 (2014).
27. Chutiwitoonchai, N. *et al.* Characteristics of IFITM, the newly identified IFN-inducible anti-HIV-1 family proteins. *Microbes Infect.* **15**, 280–290 (2013).
28. Qian, J. *et al.* Primate lentiviruses are differentially inhibited by interferon-induced transmembrane proteins. *Virology* **474**, 10–18 (2015).
29. Maréchal, V., Clavel, F., Heard, J. M. & Schwartz, O. Cytosolic Gag p24 as an index of productive entry of human immunodeficiency virus type 1. *J. Virol.* **72**, 2208–2212 (1998).
30. Sloan, R. D. *et al.* Productive entry of HIV-1 during cell-to-cell transmission via dynamin-dependent endocytosis. *J. Virol.* **87**, 8110–8123 (2013).
31. Jolly, C., Booth, N. J. & Neil, S. J. D. Cell-cell spread of human immunodeficiency virus type 1 overcomes tetherin/BST-2-mediated restriction in T cells. *J. Virol.* **84**, 12185–12199 (2010).
32. La Vega, D. M. *et al.* Inhibition of HIV-1 endocytosis allows lipid mixing at the plasma membrane, but not complete fusion. *Retrovirology* **8**, 99 (2011).
33. Ikeda, Y. *et al.* Continuous high-titer HIV-1 vector production. *Nat. Biotechnol.* **21**, 569–572 (2003).
34. Kotsopoulou, E., Kim, V. N., Kingsman, A. J., Kingsman, S. M. & Mitrophanous, K. A. A Rev-independent human immunodeficiency virus type 1 (HIV-1)-based vector that exploits a codon-optimized HIV-1 gag-pol gene. *J. Virol.* **74**, 4839–4852 (2000).
35. Kutluay, S. B. *et al.* Global changes in the RNA binding specificity of HIV-1 gag regulate virion genesis. *Cell* **159**, 1096–1109 (2014).
36. Pasquinelli, A. E. *et al.* The constitutive transport element (CTE) of Mason-Pfizer monkey virus (MPMV) accesses a cellular mRNA export pathway. *EMBO J.* **16**, 7500–7510 (1997).
37. Zhang, F. *et al.* Nef proteins from simian immunodeficiency viruses are tetherin antagonists. *Cell Host Microbe* **6**, 54–67 (2009).
38. Matheson, N. J. *et al.* Cell Surface Proteomic Map of HIV Infection Reveals Antagonism of Amino Acid Metabolism by Vpu and Nef. *Cell Host Microbe* **18**, 409–423 (2015).
39. Haller, C. *et al.* HIV-1 Nef and Vpu are functionally redundant broad-spectrum modulators of cell surface receptors, including tetraspanins. *J. Virol.* **88**, 14241–14257 (2014).
40. Fackler, O. T., d'Aloja, P., Baur, A. S., Federico, M. & Peterlin, B. M. Nef from Human Immunodeficiency Virus Type 1F12 Inhibits Viral Production and Infectivity. *J. Virol.* **75**, 6601–6608 (2001).
41. Collette, Y. & Olive, D. The primate lentivirus-encoded Nef protein can regulate several steps of the viral replication cycle. *Virology* **265**, 173–177 (1999).
42. Gummuluru, S., Kinsey, C. M. & Emerman, M. An *in vitro* rapid-turnover assay for human immunodeficiency virus type 1 replication selects for cell-to-cell spread of virus. *J. Virol.* **74**, 10882–10891 (2000).
43. Schindler, M. *et al.* Nef-mediated suppression of T cell activation was lost in a lentiviral lineage that gave rise to HIV-1. *Cell* **125**, 1055–1067 (2006).
44. Lim, E. S., Wu, L. I., Malik, H. S. & Emerman, M. The function and evolution of the restriction factor Viperin in primates was not driven by lentiviruses. *Retrovirology* **9**, 55 (2012).
45. Yount, J. S., Karssmeijer, R. A. & Hang, H. C. S-palmitoylation and ubiquitination differentially regulate interferon-induced transmembrane protein 3 (IFITM3)-mediated resistance to influenza virus. *J. Biol. Chem.* **287**, 19631–19641 (2012).
46. Jia, R. *et al.* The N-terminal region of IFITM3 modulates its antiviral activity by regulating IFITM3 cellular localization. *J. Virol.* **86**, 13697–13707 (2012).
47. Jia, R. *et al.* The C-Terminal Sequence of IFITM1 Regulates Its Anti-HIV-1 Activity. *PLoS ONE* **10**, e0118794 (2015).
48. Hach, J. C., McMichael, T., Chesarino, N. M. & Yount, J. S. Palmitoylation on conserved and non-conserved cysteines of murine IFITM1 regulates its stability and anti-influenza A virus activity. *J. Virol.* <https://doi.org/10.1128/JVI.00621-13> (2013).
49. Coller, J. & Parker, R. General Translational Repression by Activators of mRNA Decapping. *Cell* **122**, 875–886 (2005).
50. Gao, G., Guo, X. & Goff, S. P. Inhibition of retroviral RNA production by ZAP, a CCCH-type zinc finger protein. *Science* **297**, 1703–1706 (2002).
51. Zhu, Y., Wang, X., Goff, S. P. & Gao, G. Translational repression precedes and is required for ZAP-mediated mRNA decay. *EMBO J.* **31**, 4236–4246 (2012).
52. Shin, Y. C., Bischof, G. F., Lauer, W. A. & Desrosiers, R. C. Importance of codon usage for the temporal regulation of viral gene expression. *Proc. Natl. Acad. Sci. USA* **112**, 14030–14035 (2015).
53. Chang, D. D. & Sharp, P. A. Regulation by HIV Rev depends upon recognition of splice sites. *Cell* **59**, 789–795 (1989).
54. Grantham, P. & Perrin, P. AIDS virus and HTLV-I differ in codon choices. *Nature* **319**, 727–728 (1986).
55. Kypr, J. & Mrázek, J. Unusual codon usage of HIV. *Nature* **327**, 20–20 (1987).
56. Takata, M. A. *et al.* CG dinucleotide suppression enables antiviral defence targeting non-self RNA. *Nature* **550**, 124–127 (2017).
57. Reid, D. W. & Nicchitta, C. V. Diversity and selectivity in mRNA translation on the endoplasmic reticulum. *Nature Publishing Group* **16**, 221–231 (2015).
58. Li, K. *et al.* IFITM Proteins Restrict Viral Membrane Hemifusion. *PLoS Pathog* **9**, e1003124 (2013).
59. Collins, K. L., Chen, B. K., Kalams, S. A., Walker, B. D. & Baltimore, D. HIV-1 Nef protein protects infected primary cells against killing by cytotoxic T lymphocytes. *Nature* **391**, 397–401 (1998).
60. Schwartz, O., Maréchal, V., Le Gall, S., Lemonnier, F. & Heard, J. M. Endocytosis of major histocompatibility complex class I molecules is induced by the HIV-1 Nef protein. *Nat. Med.* **2**, 338–342 (1996).
61. Vendrame, D., Sourisseau, M., Perrin, V., Schwartz, O. & Mammano, F. Partial inhibition of human immunodeficiency virus replication by type I interferons: impact of cell-to-cell viral transfer. *J. Virol.* **83**, 10527–10537 (2009).
62. Jolly, C. Cell-to-cell transmission of retroviruses: Innate immunity and interferon-induced restriction factors. *Virology* **411**, 251–259 (2011).

63. Kuhl, B. D. *et al.* Tetherin restricts direct cell-to-cell infection of HIV-1. *Retrovirology* **7**, 115 (2010).
64. Casartelli, N. *et al.* Tetherin restricts productive HIV-1 cell-to-cell transmission. *PLoS Pathog* **6**, e1000955 (2010).
65. Park, H. *et al.* TAR RNA-binding protein is an inhibitor of the interferon-induced protein kinase PKR. *Proc Natl Acad Sci USA* **91**, 4713–4717 (1994).
66. Li, M. *et al.* Codon-usage-based inhibition of HIV protein synthesis by human schlafen 11. *Nature* **491**, 125–128 (2012).
67. Goodier, J. L., Pereira, G. C., Cheung, L. E., Rose, R. J. & Kazazian, H. H. The Broad-Spectrum Antiviral Protein ZAP Restricts Human Retrotransposition. *PLoS Genet.* **11**, e1005252–32 (2015).
68. Schmitz, C. *et al.* Lv2, a novel postentry restriction, is mediated by both capsid and envelope. *J. Virol.* **78**, 2006–2016 (2004).
69. Ogunkolade, B. W. *et al.* BORIS/CTCF is an RNA-binding protein that associates with polysomes. *BMC Cell Biol.* **14**, 52 (2013).
70. Yamamoto, N. *et al.* Analysis of human immunodeficiency virus type 1 integration by using a specific, sensitive and quantitative assay based on real-time polymerase chain reaction. *Virus Genes* **32**, 105–113 (2006).
71. Sloan, R. D. *et al.* Transcription of preintegrated HIV-1 cDNA modulates cell surface expression of major histocompatibility complex class I via Nef. *J. Virol.* **85**, 2828–2836 (2011).
72. Wu, Y. & Marsh, J. W. Selective transcription and modulation of resting T cell activity by preintegrated HIV DNA. *Science* **293**, 1503–1506 (2001).

## Acknowledgements

We thank Áine McKnight for helpful discussions regarding this work and Greg Towers for useful comments on this manuscript. RDS was supported as a Barts and The London School of Medicine and Dentistry Early Career Research Fellow. This work was supported by the Wellcome Trust-University of Edinburgh Institutional Strategic Support Fund. We thank Frank Kirchhoff, Paul Bieniasz, Maxine Linial, Áine McKnight, and both the NIH and NIBSC AIDS reagent programmes for the provision of reagents.

## Author Contributions

R.D.S. conceived the study. W.Y.L., R.M.F., C.L. and R.D.S. performed the experiments, analyzed data, provided reagents, or contributed towards the experimental design. W.Y.L. and R.D.S. wrote the manuscript.

## Additional Information

**Supplementary information** accompanies this paper at <https://doi.org/10.1038/s41598-018-32785-5>.

**Competing Interests:** The authors declare no competing interests.

**Publisher's note:** Springer Nature remains neutral with regard to jurisdictional claims in published maps and institutional affiliations.



**Open Access** This article is licensed under a Creative Commons Attribution 4.0 International License, which permits use, sharing, adaptation, distribution and reproduction in any medium or format, as long as you give appropriate credit to the original author(s) and the source, provide a link to the Creative Commons license, and indicate if changes were made. The images or other third party material in this article are included in the article's Creative Commons license, unless indicated otherwise in a credit line to the material. If material is not included in the article's Creative Commons license and your intended use is not permitted by statutory regulation or exceeds the permitted use, you will need to obtain permission directly from the copyright holder. To view a copy of this license, visit <http://creativecommons.org/licenses/by/4.0/>.

© The Author(s) 2018